Metamaterial Inspired Square Ring Monopole Antenna for WLAN Applications

S. Imaculate Rosaline and S. Raghavan

Department of Electronics and Communication Engineering
National Institute of Technology, Tiruchirappalli, India
imaculaterosaline@gmail.com, raghavan@nitt.edu

Abstract ─ This paper describes the design of a compact dual band monopole antenna using a metamaterial inspired split ring structure for WLAN (2.4/5.2/5.5 GHz) applications. The antenna is printed on a 20x20x0.8 mm^3 FR-4 substrate. It consists of two concentric square rings with a partial ground plane and is fed by a microstrip line. A split in the outer ring is introduced to induce magnetic resonance which in turn yields a narrow lower band resonance at 2.4 GHz. The position of the split in the ring plays a vital role in inducing the magnetic resonance. The extraction of negative permeability of the ring structure with and without the split is discussed to verify the metamaterial property existence. A prototype of the proposed structure is fabricated and the measured results comply greatly with the simulated results. The antenna has consistent radiation pattern over all the working region.

Index Terms ─ Metamaterial, monopole, negative permeability, split ring, WLAN.

I. INTRODUCTION

Wireless Local Area Network (WLAN), based on IEEE 802.11 standard operates in the 2.45 (2.4-2.48) GHz, 5.2 (5.15 -5.35) GHz and 5.8 (5.75 - 5.825) GHz frequencies. Several design of antennas capable of covering both these frequency bands are discussed in the recent past. Among the variety of antennas proposed, printed monopoles serve as a good choice because of their compactness, efficiency and easy integration with other microwave integrated circuits. Multi branched radiators [1, 2], slotted monopoles [3 - 5], meander monopoles [6], fractal shapes [7] are few among them to obtain dual band operation in the WLAN 2.5/5.2/5.8 GHz range. Recently, electromagnetic metamaterial inspired structures like split ring resonators and complementary split ring resonators are used in the design of antennas. Split ring monopole antenna proposed in [8] has impedance matching problem in the lower WLAN band, whereas the dual band antennas with CSRRs [9] and triangular split ring resonators (SRRs) [10] has larger dimensions. Recently, in [11], multiband metamaterial loaded monopole antenna is reported for WLAN/ WiMAX applications. But, yet the overall dimension of these antennas are large compared with the proposed one as shown in Table 1 below. Also, unlike these antenna analysis, this paper emphasizes on the role of metamaterial property (negative permeability) in antenna design.

Table 1: Dimensions of multiband antennas

Ref.	Dimensions, L x W (mm^2)
[8]	20 x 32
[9]	34 x 30
[10]	40 x 35
[11]	45 x 40
Proposed antenna	20 x 20

In this paper, a compact dual band monopole utilizing metamaterial inspired split ring structure is discussed. The magnetic resonance of the split ring structure offers a narrow lower band resonance at 2.4 GHz. The proposed geometry is very simple with good resonant and radiation characteristics, making it a good choice for commercial use.

II. PROPOSED ANTENNA DESIGN

The evolution of the proposed split ring radiating antenna is shown in Fig. 1. Here, configuration A shows a square ring monopole of side length 10 mm. It is fed by a 5x0.8 mm^2, microstrip line. In configuration B, a concentric inner ring is introduced to achieve resonance at the higher frequency band (5.5 GHz).

Finally, as shown in configuration C, a split is introduced along the horizontal arm of the outer ring to induce magnetic resonance and in turn yield a second lower band resonance. The antenna is printed on a 20x20x0.8 mm^3 FR-4 substrate with a relative dielectric constant of 4.4 and loss tangent of 0.002. A detailed layout of the proposed antenna is shown in Fig. 2 along with its side view and its dimensions are listed in Table 2. Photograph of the proposed structure is shown in Fig. 3.

Submitted On: November 11, 2015
Accepted On: February 20, 2016

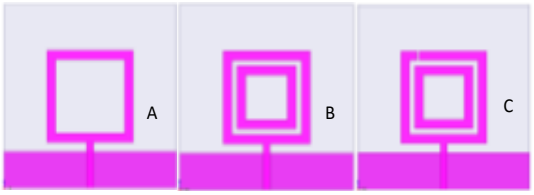

Fig. 1. Evolution of the proposed antenna.

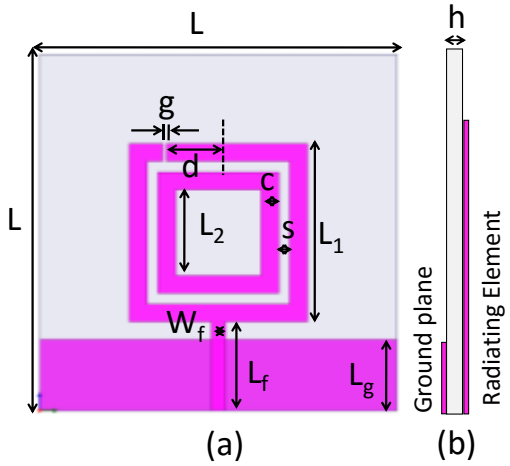

Fig. 2. Geometry of the proposed antenna: (a) top view and (b) side view.

Table 2: Dimensions of the proposed antenna

Parameter	Dimension (mm)	Parameter	Dimension (mm)
L	20	L_1	10
L_2	4.8	L_f	5
W_f	0.8	L_g	4
g	0.2	c	1
d	3	s	0.6
h	0.8		

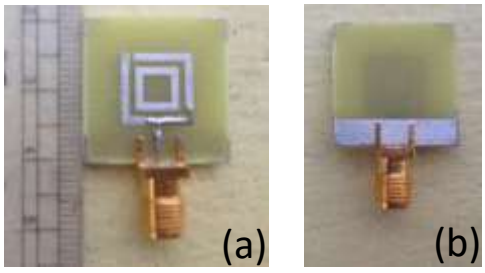

Fig. 3. Photograph of the proposed dual band antenna: (a) top view and (b) bottom view.

III. SIMULATION RESULTS

Simulations are performed using the Ansoft High Frequency Structure Simulator (HFSS) V.15.0 commercial software package. Figure 4 shows the simulated reflection coefficient characteristics of the three configurations shown in Fig. 1. Configuration A shows resonance around 6 GHz for W_f = 0.8 mm. When the inner concentric ring is introduced as shown in configuration B, the impedance matching at 6 GHz is improved, since the inner ring by itself exhibits a quarter wavelength resonance for the radii of 6.8 mm. Now, when the split is introduced along the outer ring (configuration C), the current along this path gets perturbed, and leads to a lower band resonance around 2.4 GHz. Figure 5 shows the parametric study on W_f for configuration B. It is inferred that when W_f is 1.6 mm, resonance around 4 GHz is observed and when W_f is 0.8 mm, resonance around 6 GHz is observed. Hence, for fabrication, W_f = 0.8 mm is chosen. The proposed structure shows a dual band resonance centred at 2.4 GHz, and 5.5 GHz, with -10 dB impedance bandwidth of 150 MHz (2.35 – 2.5 GHz) and 1230 MHz (4.9 – 6.13 GHz). Here, the position of the split from its centre (d) plays an important role in determining the lower resonant band. This is validated by performing a parametric study. Figure 6 shows the parametric study on the position 'd' of the split ring from the centre. It is noted that, when the split is present at the centre, there is no lower band resonance and when the split is moved on either side at a distance of 1 mm, 2 mm, etc. from the centre, a narrow lower band resonance around 2.4 GHz is inferred. This is due to the induced charge concentration around the split gap. Simulated surface current distribution of the proposed antenna at 2.4 GHz and 5.5 GHz are shown in Figs. 7 (a) and (b). It is inferred that, for 2.4 GHz band, the current is dense along the longest arm of the outer ring and for 5.5 GHz, the current is distributed along the outer ring. The coupling of current to the inner ring can also be noticed. Figure 7 (c) shows the simulated electric field distribution at 2.4 GHz. A dense charge distribution around the split gap is inferred.

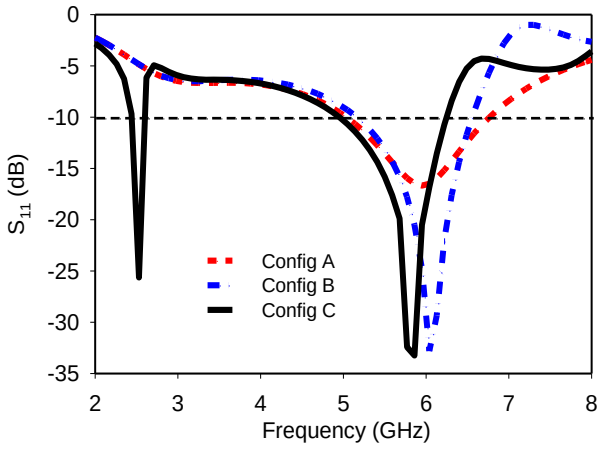

Fig. 4. Simulated input reflection coefficient characteristics of configuration A, B and C.

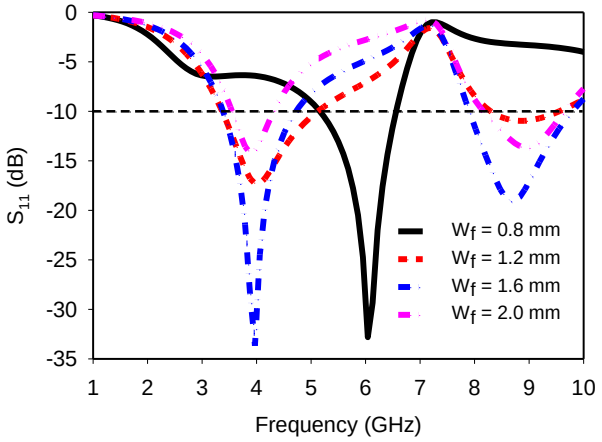

Fig. 5. Simulated input reflection coefficient characteristics of configuration B for various feed width Wf.

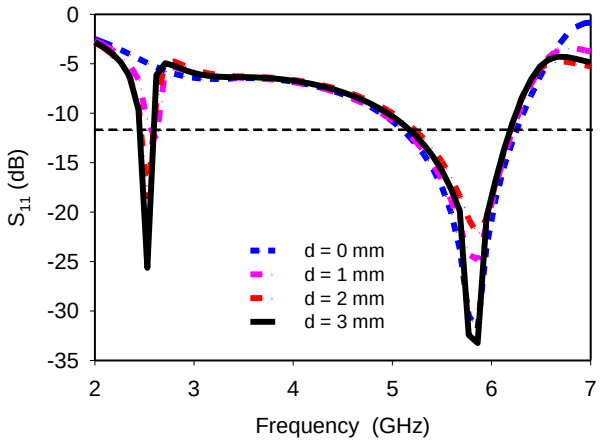

Fig. 6. Simulated input reflection coefficient characteristics of configuration C for various distance of the split, d, from the center.

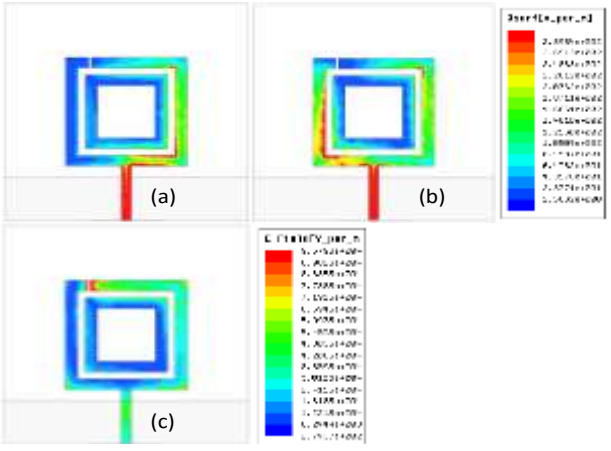

Fig. 7. Simulated surface current distribution of the proposed antenna at: (a) 2.4 GHz, (b) 5.5 GHz, and (c) simulated electric field distribution at 2.4 GHz.

IV. MEASUREMENT RESULTS

The return loss characteristics are measured using a vector network analyser. Figure 8 shows the simulated and measured reflection coefficient characteristics of the proposed antenna. The measured data exhibits a dual band resonance at 2.4 GHz, and 5.5 GHz, with -10 dB impedance bandwidth of 150 MHz (2.35 – 2.5 GHz) and 1600 MHz (4.9 – 6.5 GHz). The measured results greatly comply with the simulated results in the 2.4 GHz band; however, a discrepancy in the higher operational band at 5.5 GHz is observed. This may be attributed to fabrication tolerance and thick soldering of SMA connector. Figure 9 shows the measured radiation pattern of the proposed antenna at 2.4 GHz, 5.2 GHz and 5.8 GHz. A consistent omnidirectional pattern is observed in the H plane and a bidirectional pattern is observed in the E plane over all the operating region. A peak gain of 1.6 dBi and 2.8 dBi are inferred around 2.4 GHz and 5.5 GHz during measurement. Thus, the radiation and resonant behaviour of the antenna are found satisfactory making the antenna suitable for wireless communication devices.

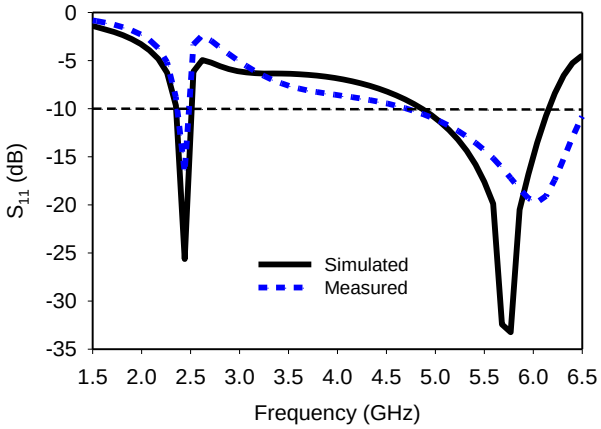

Fig. 8. Simulated and measured input reflection coefficient characteristics of the proposed antenna.

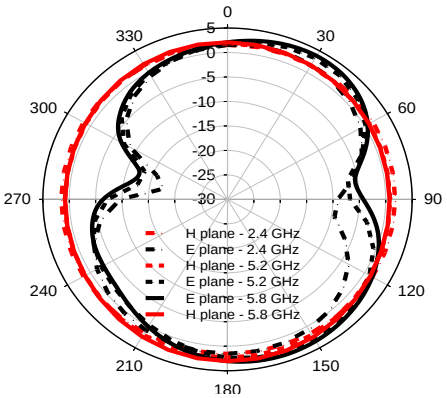

Fig. 9. Measured H plane and E plane pattern of the proposed antenna at 2.4 GHz, 5.2 GHz and5.8 GHz.

V. SPLIT RING ANALYSIS

The radiating element by itself is a split ring structure. The structure is analysed using the classic waveguide theory approach in which the structure is placed inside a waveguide and an EM wave is passed through one of its ports and measured through the other port. The transmission and reflection coefficients are noted and from which the effective material parameters (permeability and permittivity) are extracted [12]. Figure 10 shows the real parts of extracted effective permeability values for the two split ring structure with and without the split gap. It is inferred that the permeability is negative around 2.4 GHz for the structure with split and a constant permeability for the structure without the split, which confirms the metamaterial property existence.

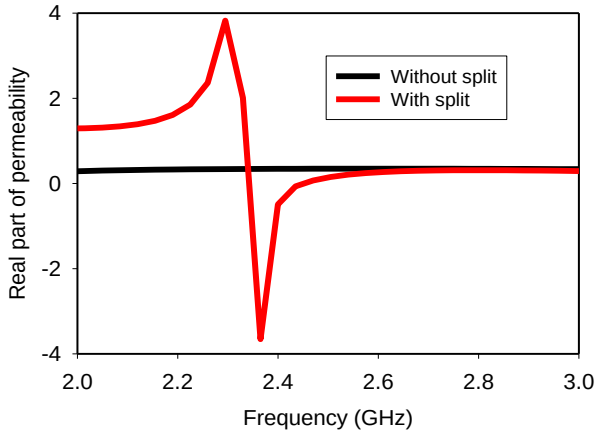

Fig. 10. Real part of extracted effective permeability of the two split ring structures.

VI. CONCLUSION

A dual band monopole antenna suitable for WLAN 2.4/5.5 GHz applications is presented in this paper. The antenna makes use of a metamaterial inspired split ring structure for achieving the dual band resonance. The antenna geometry is very simple and also compact making mass production easy. The radiation pattern and gain are consistent over all the operating bands making the proposed antenna a good choice for wireless applications.

REFERENCES

[1] Y. Xu, Y.-C. Jiao, and Y.-C. Luan, "Compact CPW-fed printed monopole antenna with triple band characteristics for WLAN/WiMAX applications," *Electron Lett*., vol. 48, pp. 1519-1520, 2012.

[2] X. L. Sun, L. Liu, S. W. Cheung, and T. I. Yuk, "Dual-band antenna with compact radiator for 2.4/5.2/5.8 GHz WLAN applications," *IEEE Trans. Ant. P*, vol. 60, pp. 5924-5931, 2012.

[3] W.-C. Liua, C.-M. Wua, and N.-C. Chu, "A compact low profile dual-band antenna for WLAN and WAVE applications," *AEU Int. J. Electron. C*, vol. 66, pp. 467-471, 2012.

[4] C.-Y. Huang and E.-Z. Yu, "A slot monopole antenna for dual band WLAN applications," *IEEE Antennas Wireless Propag. Lett.*, vol. 10, pp. 500-502, 2011.

[5] X.-Q. Zhang, Y.-C. Jiao, and W.-H. Wang, "Compact wide tri-band slot antenna for WLAN/WiMAX applications," *Electron. Lett*., vol. 48, pp. 64-65, 2012.

[6] H.-Y. Chien, C.-Y.-D. Sim, and C.-H. Lee, "Dual band meander monopole antenna for WLAN operation in laptop computer," *IEEE Antennas Wireless Propag. Lett*., vol. 12, pp. 694-697, 2013.

[7] R. Ghatak, R. K. Mishra, and D. R. Poddar, "Perturbed Sierpinski carpet antenna with CPW feed for IEEE 802.11 a/b WLAN application," *IEEE Antennas Wireless Propag. Lett*., vol. 7, pp. 742-744, 2008.

[8] S. C. Basaran and Y. E. Erdemli, "A dual band split ring monopole antenna for WLAN applications," *Microw. Opt. Technol. Lett*., vol. 51, pp. 2685-2688, 2009.

[9] S. C. Basaran, U. Olgun, and K. Sertel, "Multiband monopole antenna with complementary split ring resonators for WLAN and WiMAX applications," *Electron. Lett*., vol. 49, pp. 636-638, 2013.

[10] K. Yang, H. Wang, Z. Lei, Y. Xie, and H. Lai, "CPW-fed slot antenna with triangular SRR terminated feed line for WLAN/WiMAX applications," *Electron. Lett*., vol. 47, pp. 685-686, 2011.

[11] H. He, Y. Liu, S. Zhang, and S. Gong "Multiband metamaterial-loaded monopole antenna for WLAN/WiMAX applications," *IEEE Antennas Wireless Propag. Lett*., vol. 14, pp. 662-665, 2015.

[12] D. R. Smith, S. Schultz, P. Markos, and C. M. Soukoulis, "Determination of effective permittivity and permeability of metamaterials from reflection and transmission coefficients," *Phys. Rev. B*, vol. 65, pp. 195104-195109, 2002.